Detection of Slump Slides on Earthen Levees Using Polarimetric SAR Imagery

James V. Aanstoos, Khaled Hasan, Charles G. O'Hara, Lalitha Dabbiru, Majid Mahrooghy, Rodrigo Nobrega, Matthew A. Lee

Geosystems Research Institute
Mississippi State University
Mississippi State, MS 39762 USA
j.aanstoos@ieee.org

***Abstract*—Key results are presented of an extensive project studying the use of synthetic aperture radar (SAR) as an aid to the levee screening process. SAR sensors used are: (1) The NASA UAVSAR (Uninhabited Aerial Vehicle SAR), a fully polarimetric L-band SAR capable of sub-meter ground sample distance; and (2) The German TerraSAR-X radar satellite, also multi-polarized and featuring 1-meter GSD, but using an X-band carrier. The study area is a stretch of 230 km of levees along the lower Mississippi River. The L-band measurements can penetrate vegetation and soil somewhat, thus carrying some information on soil texture and moisture which are relevant features to identifying levee vulnerability to slump slides. While X-band does not penetrate as much, its ready availability via satellite makes multitemporal algorithms practical. Various feature types and classification algorithms were applied to the polarimetry data in the project; this paper reports the results of using the Support Vector Machine (SVM) and back-propagation Artificial Neural Network (ANN) classifiers with a combination of the polarimetric backscatter magnitudes and texture features based on the wavelet transform. Ground reference data used to assess classifier performance is based on soil moisture measurements, soil sample tests, and on site visual inspections.**

Keywords-synthetic aperture radar, levee screening, earthen levees, UAVSAR, TerraSAR-X

I. INTRODUCTION

In the United States alone, more than 150,000 kilometers of earthen levee structures of varying designs and conditions protect large areas of populated areas from flooding. The potential for loss of life and property associated with catastrophic failure of such levees can be quite large.

Currently, limited resources for inspections of this infrastructure prevent adequate monitoring to achieve desirable risk management levels. There is a need to prioritize the allocation of these resources in a cost-efficient manner. Levee managers and federal agencies will benefit from any tools allowing them to assess levee health rapidly with robust techniques that identify, classify and prioritize levee vulnerabilities with lower costs than traditional programs not based on the use of remote sensing. This paper presents results from an extensive project studying the use of synthetic aperture radar (SAR) as an aid to the levee screening process. The remote sensing data included two SAR sources:

(1) The NASA UAVSAR (Uninhabited Aerial Vehicle SAR), a fully polarimetric L-band SAR which is also designed to acquire airborne repeat track SAR data for differential interferometric measurements. This instrument is capable of sub-meter ground sample distance.

(2) The German TerraSAR-X satellite with its X-band multi-polarimetric SAR and high spatial resolution

The longer-wavelength L-band SAR measurements can penetrate vegetation and even the top layer of soil, depending on moisture content. On that basis this wavelength was selected for our study under the assumption that the backscatter will carry information from the top layer of the soil that will be valuable in detecting changes in levees that will be key inputs to a levee vulnerability classification system.

The TerraSAR-X satellite provides advantages of better temporal resolution and lower cost of data acquisitions than an airborne platform in general, and also high spatial resolution. The shorter wavelength however results in less penetration depth, especially in the presence of vegetation such as trees, shrubs and grass, thus reducing the amount of information about the soil present in the backscatter. However, some variations in the vegetation itself may be related to levee vulnerabilities, mitigating this disadvantage of the shorter wavelength option. Furthermore, changes in surface roughness are easier to detect with shorter wavelengths, and this characteristic is relevant to our targets of interest.

Our test study area is a stretch of 230 km of levees along the lower Mississippi River, along the western boundary of the state of Mississippi. One type of problem that occurs frequently along these levees, which can be a precursor to levee failure during a high water event, is the slump slide.

Slump (or slough) slides along a levee are slope failures, which leave areas of the levee vulnerable to seepage and failure during high water events [1]. A photograph of a typical slump slide, in this case one which appeared during the recent spring 2011 flooding of the Mississippi River, is shown in Fig. 1. The roughness and related textural characteristics of the soil in a slide affect the amount and pattern of radar backscatter. The type of vegetation that grows in a slide area often differs from the surrounding levee vegetation, which can also be utilized in detecting slides [2].

Funded in part by Department of Homeland Security Southeast Region Research Initiative (SERRI) at Department of Energy's Oak Ridge National Laboratory, and by NASA's Applied Sciences Program

Fig. 1. Typical levee slough (or slump) slide. This one appeared during the major flood event in the Spring of 2011

Early detection of the occurrence of such slides could help levee mangers prioritize their inspection and repair efforts. A remote sensing based solution for their rapid detection would be more efficient and cost effective than frequent on-site visits. Furthermore, it may be possible to detect less obvious precursors to slides and boils by sensing characteristics of the surface soils and vegetation. A working hypothesis of this study was that such characteristics will be manifested in the backscatter of polarimetric radar due to its response to spatially variant soil moisture. For example, L band radar is known to penetrate soil to various depths depending on its moisture content, and has been used to map surface soil moisture [3].

II. DATA

A. UAVSAR Data

This study used data from the NASA Jet Propulsion Laboratory's UAVSAR (Uninhabited Aerial Vehicle Synthetic Aperture Radar) instrument, a polarimetric L-band synthetic aperture radar flown on a Gulfstream-3 research aircraft. The salient characteristics of this instrument are shown in Table I.

The UAVSAR is normally flown at an altitude of 12.5 km and takes an image swath 20 km wide. Our study area was designed to be imaged in two straight-line flight segments structured to capture most of the river levees on both sides of the river. The study area is shown in Fig. 2, with a color composite representation of the radar data overlaid on a base map of the vicinity. A total of five UAVSAR data collections have been made: (1) June 16, 2009; (2) January 25, 2010; (3) April 28 2010; (4) June 7, 2011; and (5) June 22, 2011. The higher frequency of flights during the spring of 2011 was driven by the 100-year level flood event occurring at that time, which created a valuable opportunity for collecting data at very high-water levels. The flights were flown in a "racetrack" pattern looking toward the river from opposite directions, in order to achieve a range of local incidence angles along the levees.

Although the raw ground sample distance is 1.6 by 0.6 meters, most of our efforts use the multi-look 5 by 7 meter data to minimize speckle effects.

TABLE I. UAVSAR SPECIFICATIONS [4]

Parameter	Value
Frequency	L-band
Bandwidth	80 MHz
Range Resolution	1.8 m
Polarization	Full quad polarization
Quantization	12 bits
Antenna size	0.5 m range/1.5 azimuth
Power	> 2.0 kW

Fig. 2. Study area with radar color composite image overlaid on base map. Radar swath is 20 km wide and total length is 230 km of the lower Mississippi River valley bordering Arkansas, Mississippi, and Lousisiana.

B. *Satellite Data*

In addition to UAVSAR, data from the German TerraSAR-X satellite was acquired over portions of the same study area. Characteristics of this sensor are shown in Table II. Due to the relatively low cost (for TerraSAR-X Science Team members), we acquired a large number of such scenes over a great variety of seasons and time periods. By the end of the project a total of 56 TerraSAR scenes had been acquired. The locations and scene sizes relative to the UAVSAR image swath are shown in Fig. 3.

TABLE II. TERRASAR-X SPECIFICATIONS [5]

Parameter	Value
Radar Carrier Frequency	9.65 GHz (X-band)
Bandwidth	150 MHz
Pulse Repetition Frequency	2 – 6.5 KHz
Incidence Angle Range	20° - 45°
Polarization	HH, HV, VH, VV
Nominal altitude	514 km
Revisit time	11 days
Power	> 2.0 kW

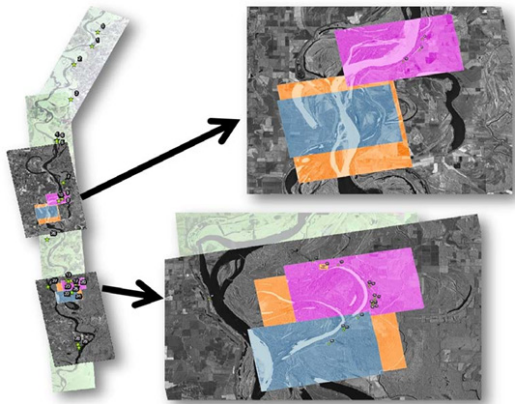

Fig. 3. Location of TerraSAR-X satellite SAR scenes in relation to the larger UAVSAR image swath.

C. *Ancillary and Reference Data*

Ancillary data can be used to assist the levee classification process in addition to the remote sensing data. This includes knowledge of the soil characteristics in the vicinity of the levees, the underlying geology of the area, and history of past problems and inspections of the levees.

Reference (or "ground truth") data is obtained for the purpose of training the supervised classification algorithms and testing and validation of results. Such data fall into two major categories: (1) known levee vulnerability points such as slump slides, seepage points, or sand boils; and (2) measured soil properties such as moisture content, sand/clay ratios, etc. The former category is collected with the assistance of the US Army Corps of Engineers (USACE), which maintains a history of past problems and has identified particularly problematic sections of levees in the study area. A challenge in using this data is that once USACE identifies problems it soon repairs them, depending on their severity. This leaves the targets of interest in their natural (un-repaired) state for a limited period of time, making the number of such targets available during a given remote sensing data acquisitions relatively small. On the assumption that the soil properties in the vicinity of such problems may have similar characteristics which may be detectable in the radar signatures, we use some of these repaired locations in our training data, and plot their locations along with the unrepaired targets when analyzing results.

The second category of reference data-- measured soil properties-- was collected in a number of ways. We made direct measurements of soil moisture (volumetric water content (%VWC) using handheld probes during each radar flight or satellite overpass. We focused these collections on specific areas of interest (AOIs) within the large study are, which included slide and non-slide ("healthy") regions. In addition we contracted with a company (Soil and Topography Information, LLC) that performs intelligent sampling collection of soil property measurements using vehicle-based probes that allow a large collection area to be sampled efficiently. We measured in this manner soil properties over a 3-mile long section of the study area levees, divided into 3 one-mile long AOI's. Two of these were in regions of frequent slump slide activity and the third was a "healthy" levee section having no history of slides. An example of this data is shown in Fig. 4, which plots the spatial distribution of one variable: sub-surface soil moisture. The mean values of this and other of the measured soil properties, including surface moisture, clay fraction, and sand fraction, were computed for each of the 3 AOIs, and are shown in Fig. 5. Notably, the healthy AOI showed significantly lower moisture levels and higher sand fraction than either of the other two AOIs. These differences could potentially influence the relative magnitudes and spatial distribution of the polarimetric SAR backscatter channels, thus supporting the ability to use features based on them in a levee classification application.

III. METHODS

Features believed to provide good potential for discrimination of the targets of interest were designed,

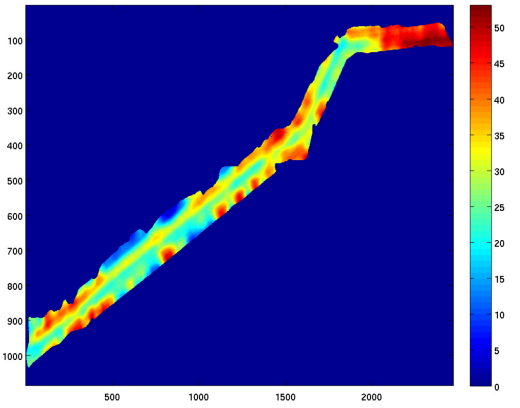

Fig. 4. Example of in-situ soil properties data: soil moisture along levees

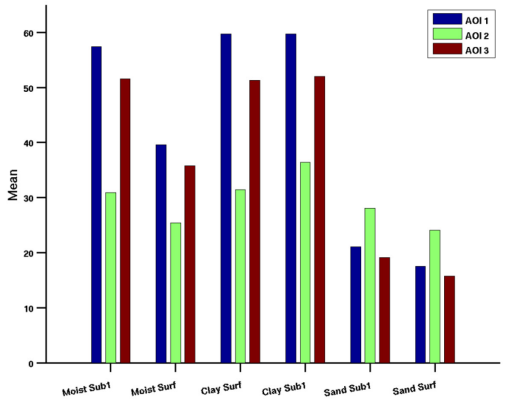

Fig. 5. Mean values of soil moisture and clay/sand percentages measured in situ for 3 different areas of inerest along the levee. AOI 2 (green) is the "healthy" segment.

computed, and tested. Both per-pixel and window-based (textural) features were examined. The candidate features were tested with our training data to determine separability between classes of interest. Over 144 features in total were investigated, including radiometric and textural features. Classification algorithms tested and reported here include a back-propagation Artificial Neural Network (ANN) and the Support Vector Machine (SVM) method.

Stepwise Linear Discriminant Analysis (S-LDA) [6] was employed for feature reduction and optimization. In this approach, various features derived from the SAR backscatter imagery are concatenated into a vector, and a forward-selection, backward rejection technique is employed to prune away features that are "less" relevant to the classification problem at hand. S-LDA reduces the feature set by selecting a subset of all available features based on a metric that quantifies the class separation provided by each feature. In this study Bhattacharyya Distance (BD) was used as the metric for calculating the class separation. An LDA based feature "optimization" is then employed on this reduced dimensional subset of features identified by the forward selection, backward rejection search. S-LDA is hence extremely valuable in ensuring that the "most" relevant features are provided to the classifier while ensuring that the classifier is not over-burdened by an excessively high dimensional feature space. The "classifier" employed in this work to model class-specific information and label test data (pixels) appropriately was the popular maximum-likelihood classifier. This classifier assumes Gaussian probability distribution functions for each class, and uses training data to learn the mean vector and covariance matrix per class. This information is then employed to find the distance of test vectors from each class model, and a class label is assigned to the sample that maximizes the likelihood value of the test sample being in that class. We used SLDA in this way to narrow the size of the feature set within a class of features (such as radiometric, GLCM, or Wavelet), but then experimented with various combinations of each reduced-size feature set in different classifiers.

Features included in this study are described in detail below. These include per-pixel intensity related features, as well as features extracted within a window around each pixel – known as textural features.

A. Per-pixel Features

The polarimetric radar data contain three independent channels of backscatter coefficients, those for like-polarized (HH, VV) and cross-polarized (HV) combinations of transmitted and received polarizations. For each, we get complex values giving both magnitude and phase information. The magnitudes of these channels can be used as basic per-pixel features with any classifier. For the airborne UAVSAR radar data we have two different views of the same levees from opposite directions and have used the 3 channels from each direction for each pixel in case there is additional information due to the great difference in local incidence angles.

The relationship between the complex backscatter coefficients can reveal details on the nature of the scattering mechanism of the targets, such as relative amount of surface, double-bounce, or volume scattering. Decompositions of parameters derived from 2 or 3 of the polarimetric channels have also been used as classification features [10]. We previously investigated the use of such decompositions for the levee screening application [11].

B. Textural Features

In addition to the per-pixel backscatter features, a number of texture features were explored which utilize the values from pixels in a neighborhood around each pixel being analyzed. Features based on the Gray Level Co-occurrence Matrix (GLCM) [7] and on the discrete wavelet transform (DWT) [10], showed promising results. We previously reported results of our work using the GLCM features [12].

The ability of wavelet analysis to decompose an image into different frequency sub-bands makes it suitable for image classification [9]. In some applications, the energy of each sub-band is used as a texture feature. In others, a feature selection analysis chooses a subset of these which prove effective for a given texture-based classification. Other parameters to be determined include the choice of mother wavelet function, and the neighborhood window size.

For our application, we used wavelet features with one decomposition level from each of the radar polarization channels. We tested these features using different sliding window sizes (5, 7, 8, and 9) and mother wavelets (Daubechies, Haar, Symlet, and Biorthogonal) and selected those that maximize the separation of the targets of interest from the background. The Daubechies mother wavelet was chosen, and a window size of 7.

C. Classification Algorithms

A back propagation neural network (BPNN) is a multilayer, feed-forward artificial neural network trained by the back propagation method. It is defined by a network of input, output, and hidden layers as depicted in Fig. 6. The X_i are the values of the input features; Z_i are the values at the (one or more) hidden layers; W is a vector of weights applied to the hidden layer(s); and V the vector of weights applied to the

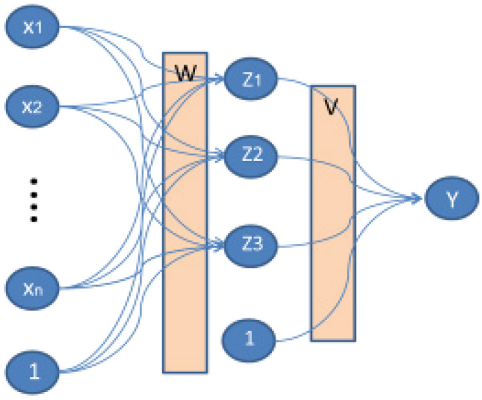

Fig. 6. Back propagation neural network with one hidden layer.

output layer. The weights are set iteratively in training mode using the error back-propagation method after measuring errors resulting from presenting training data to the network. We used a network with two hidden layers, and the inputs were the polarimetric backscatter magnitudes and the selected wavelet features.

We also tested the Support Vector Machine (SVM) method. SVM is a powerful supervised learning method for analyzing and recognizing patterns. It discriminates between two classes by fitting an optimal separating hyperplane to the training data within a multidimensional feature space. The advantage of SVM is that it works well with small training datasets, so is particularly appropriate for our levee slide application. In this method, the input data are first transformed into a feature space (possibly with a higher dimension than the original data), either linearly or non-linearly, based on a kernel function. Next, a hyperplane which separates the classes is computed by applying an optimization method.

The SAR backscattering coefficients and wavelet features computed from them were used as features input to the classifier. A Gaussian radial basis kernel was used and the training process involved the estimation of the kernel parameter γ and the regularization parameter C. To simplify the parameter selection, the datasets were normalized before the classifier training and optimal parameters for γ and C were defined. The accuracy of the classification varies with the γ parameter and its selection is discussed along with the results below.

IV. Results

Results of this study show great promise, with high accuracies for detection of active slump slides on earthen levees. However, the number of training sites was very limited and further experiments are needed to validate these results. All of the tests reported here used both the wavelet and backscatter features. We tested the UAVSAR data in both an ANN and an SVM classifier, and also tested SVM with the TerraSAR-X satellite data. Unfortunately the satellite and airborne radar acquisitions were not close enough in time that we were able to use the same training data for each.

Fig. 7 shows the results of using the back propagation ANN with UAVSAR data. The backscattering coefficients HH, HV and VV and wavelet features computed from them are used as features input to the classifier. The neural network designed has two hidden layers with three neurons in the first hidden layer, and eight in the second layer. The training data were fed into the input layer and propagated through the hidden layer to the output layer. The number of iterations was set to 500. The differences between the computed and desired outputs were computed and fed backwards to adjust the network. The algorithm adjusts the weights of each connection in order to reduce the value of the error function. The overall accuracy achieved with this classifier was 94%. Table III depicts the confusion matrix of the classification.

TABLE III. Confusion Matrix for BPNN Classifier.

	Slide	Healthy	Accuracy
Slide	38	3	0.93
Healthy	3	65	0.96
Accuracy	0.93	0.96	0.94

The SVM classifier was also used with UAVSAR backscattering coefficients HH, HV and VV and wavelet features computed from them. It was tested with the same training data and study area. A Gaussian radial basis kernel was used and the training process involved the estimation of the kernel parameter γ and the regularization parameter C. To simplify the parameter selection, the datasets were normalized before the classifier training and optimal parameters for γ and C were defined. Since the accuracy of the classification varies with the γ parameter, the relationship between accuracy and γ sampled over the range 0.03 – 0.1 was defined for the analysis and plotted in Fig. 8 along with the classification map. The results show that SVM performed very well with a highest accuracy of 100% for the slide detection and 93% for the healthy levee mapping.

With such high performance on the UAVSAR data, we tested the SVM algorithm with similar features computed from the TerraSAR-X data. That data was only available with two polarization channels, HH and VV. These backscattering coefficients and the wavelet features derived from them were used as inputs to the classifier. It was tested in a nearby portion of the levee area used to test the UAVSAR data; however only one active slide was available. The masks used for training are shown in Fig. 9.

Fig. 10 shows the results of running this classification method over the area of study. Pixels classified as healthy (non-slide) are in green, and those classified as slide pixels are in blue. It can be seen that the actual slide area was well-detected, but there are a number of false positives detected as slides among the actual healthy areas. The density of these can be seen to be much lower than the true positives, thus.

Fig. 11 shows how the accuracy of this SVM classifier is affected by the quantity of training samples used. This type of sensitivity analysis is useful in determining the minimum number of training samples needed to achieve a reasonable accuracy. In this case, it can be seen that accuracy levels off at a quite high level of 90% with around 50 training samples.As has been stated, these results are still preliminary and cannot

yet be rigorously assessed or validated until more samples are tested.

V. Conclusions and Future Work

The results show that high accuracies for detection of slump slides on levees can be achieved with multi- polarization SAR data, both 3-channel L-band SAR as well as from 2-channel X-band SAR. However, due to the limited availability of active slides during the test period, these conclusions need more rigorous testing with a greater variety of samples and locations. Furthermore, the locations and distribution of pixels identified as false positives present the intriguing possibility that there may be useful information about soil properties that could lead to potential future slide activity.

It is recommended that anomalies detected by classifiers be thoroughly investigated by experts using such methods as soil bore samples to determine if they are really false positives or not—such sites might have soil properties that could lead to instability and thus future slide and seepage activity, and the ability to detect them remotely prior to the actual slide would be quite valuable.

Both the airborne and satellite based instruments used in this study can also be used with interferometric SAR methods to derive surface deformation maps, which can be valuable inputs to a levee screening process. We examined some interferograms from our data, but they suffered from high levels of decorrelation and lack of sufficient persistent scatterers to be useful. Such limitations can be overcome to some extent by averaging over many more time samples, and we plan to do this in the future.

Acknowledgment

The authors acknowledge the contributions of two partnering organizations in this research: The US Army Corps of Engineers, and Soil and Topography Information, LLC.

References

[1] J. Dunbar, “USACE’s lower Mississippi valley engineering geology and geomorphology mapping program for levees,” presentation at Vicksburg, MS, April 16, 2009.

[2] A. K. M. A. Hossain, G. Easson, K. Hasan, “Detection of Levee Slides Using Commercially Available Remotely Sensed Data”, Environmental and Engineering Geoscience, v.12; no. 3; pp. 235 – 246, 2006.

[3] Jiancheng Shi, J. Wang, A. Hsu, P. O’Neill, E.T. Engman, “Estimation of bare soil moisture and surface roughness parameter using L-band SAR image data," IEEE Trans. Geoscience Remote Sensing, Vol. 35, No. 5, 1254-1266, 1997

[4] Kevin Wheeler, Scott Hensley, Yunling Lou, Tim Miller, Jim Hoffman, "An L-band SAR for repeat pass deformation measurements on a UAV platform", 2004 IEEE Radar Conference, Philadelphia, PA, April 2004.

[5] Aanstoos, J.V., Hasan, K., Mahrooghy, M., Dabbiru, L., Nobrega, R. A. A., & Prasad, S. Screening of Earthen Levees Using TerraSAR-X Radar Imagery. 4th TerraSAR-X Science Team Meeting. Oberpfaffenhofen, Germany: DLR (German Aerospace Center), February 2011.

[6] R. O. Duda, P. E. Hart and D. G. Stork, *Pattern Recognition*, 2nd ed. ed. Hoboken, NJ: Wiley-Interscience, 2000.

[7] R.M. Haralick, K. Shanmugam and I. Dinstein. "Textural features for image classification," IEEE Trans. Syst. Man Cybern. 3 (1973), pp. 610–621.

[8] C. S. Burrus, R. A. Gopinath, H. Guo, Introduction to Wavelets and Wavelet Transforms: A Primer, Prentice Hall, August 24, 1997.

[9] Huang, K., Aviyente, S., "Wavelet Feature Selection for Image Classification," Image Processing, IEEE Transactions on, vol.17, no.9, pp. 1709-1720, Sept. 2008.

[10] Cloude, Shane Robert and Eric Pottier, “A review of target decomposition theorems in radar polarimetry”, *IEEE Transactions on Geoscience and Remote Sensing,* vol. 34, No. 2, 1996

[11] Dabbiru, L., and J. V. Aanstoos (2010). “Classification of Levees Using Polarimetric Synthetic Aperture Radar (SAR) Imagery,” in Proceedings of the 2010 39th IEEE Applied Imagery Pattern Recognition Workshop, Washington, DC: IEEE.

[12] Lee, M., Aanstoos, J.V., Bruce, L.M., & Prasad, S. (Jul 2012). Application of Omni-directional Texture Analysis to SAR Images for Levee Landslide Detection. IEEE Geoscience and Remote Sensing Society IGARSS 2012, Munich, Germany: IEEE.

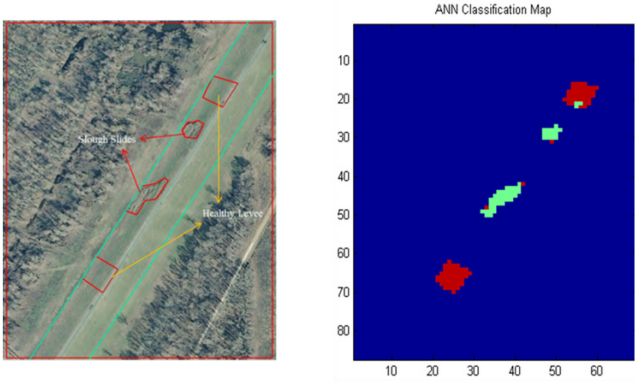

Fig. 7. Back propagation neural network result. (a) Optical image of the subset with training masks for slide and healthy pixels. (b) Back Propagation Neural Network classification result (blue = background, green = slide, red = healthy levee).

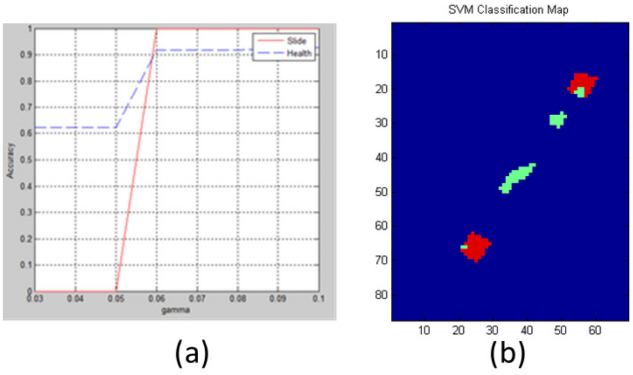

Fig. 8. SVM classification results with UAVSAR data. (a) The relationship between classification accuracy and γ with a constant regularization parameter log C = 4 for slide (red line) and healthy classes. (b) Training Mask for slide and healthy pixels. (c) SVM classification map.

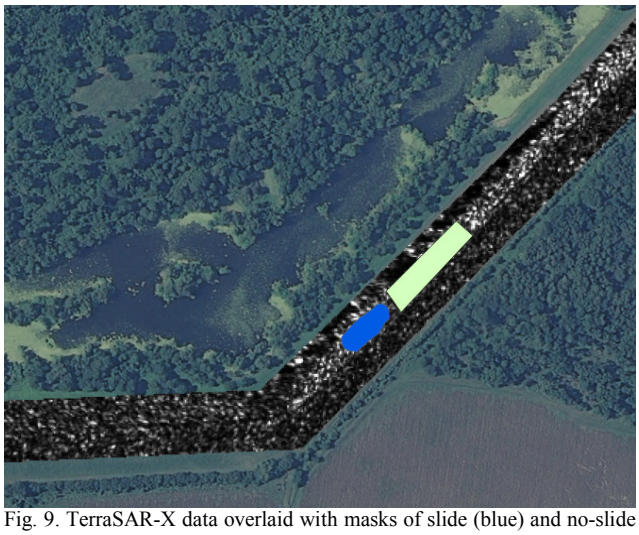

Fig. 9. TerraSAR-X data overlaid with masks of slide (blue) and no-slide (green) areas.

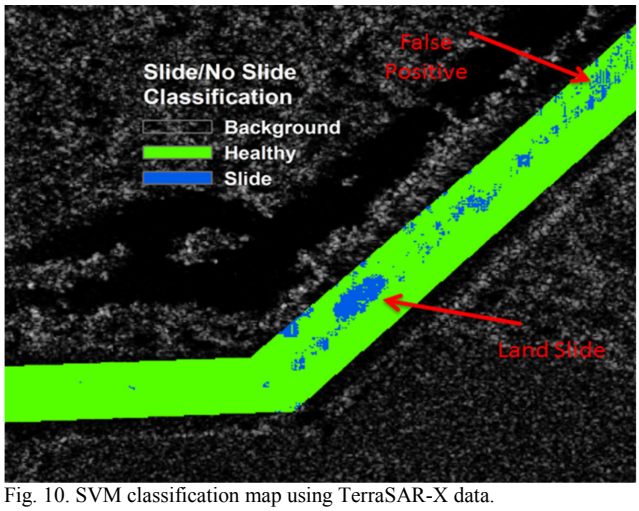

Fig. 10. SVM classification map using TerraSAR-X data.

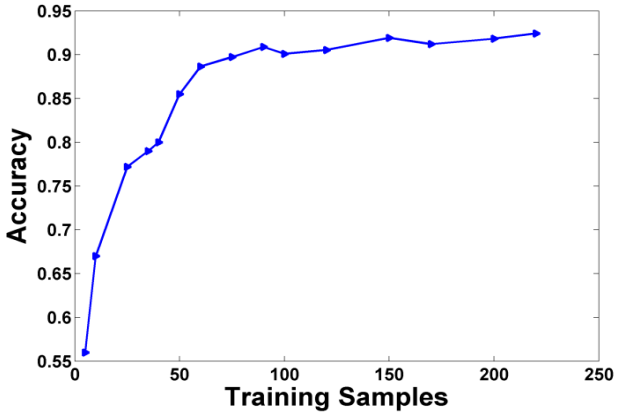

Fig. 11. SVM classification accuracy using TerraSAR-X data, versus number of training samples.